

A role for actin-driven secretion in auxin-induced growth

F. Waller, M. Riemann, and P. Nick*

Institut für Biologie II, Albert-Ludwigs-Universität Freiburg, Freiburg

Received May 17, 2001

Accepted July 21, 2001

Summary. In epidermal cells of *Zea mays* coleoptiles, actin microfilaments are organized in fine strands during cell elongation, but are bundled in response to signals that inhibit growth. This bundling response is accompanied by an increased membrane association of extracted actin. Brefeldin A, an inhibitor of vesicle secretion, increases the membrane association of actin, causes a bundling of cortical actin microfilaments, and reduces the sensitivity of cell elongation to auxin. A model is proposed where auxin controls the dynamics of an actin subpopulation that guides vesicles loaded with components of the auxin-signaling machinery towards the cell poles.

Keywords: Actin; Auxin; Brefeldin A; Coleoptile; *Zea mays*; Vesicle transport.

Introduction

The stimulation of cell elongation in graminean coleoptiles has been the classical response to study the action of the plant hormone auxin. Auxin causes a loosening of the epidermal cell wall that limits the expansion of the subtending tissues (Kutschera et al. 1987). There exist several mechanisms that have been discussed in the context of auxin-induced growth ranging from auxin-induced proton excretion (Rayle and Cleland 1992) over synthesis of proteins that cleave hydrogen bonds between the cellulose microfibrils (Cosgrove and Li 1993) to the breakdown of specific polysaccharides that presumably control the extensibility of the cell wall (McDougall and Fry 1988).

In addition to these mechanisms that are affecting the biochemical composition of the cell wall, auxin can stimulate growth by inducing structural changes. In the

presence of auxin, cellulose microfibrils are deposited in transverse orientation at the outer epidermal wall (Bergfeld et al. 1988), reinforcing cell expansion in the long axis of the cell. The deposition in transverse orientation is replaced by a longitudinal orientation of cellulose synthesis when the coleoptiles are depleted from endogenous auxin. This auxin-dependent directional switch of cellulose deposition is based on a corresponding change in the direction of cortical microtubules (Nick et al. 1990) underneath the outer epidermal wall. These microtubules serve as guiding tracks for the movement of cellulose-synthesizing enzyme complexes residing in the plasma membrane (Giddings and Staehelin 1991) and are responsible for stable, long-lasting changes of growth (Nick and Schäfer 1994). However, fast growth responses such as phototropic bending can occur in the absence of cortical microtubules (Nick et al. 1991).

Such microtubule-independent growth responses are not isodiametric but involve a clear axis of growth. This means that they must be based on mechanisms that embody some kind of directionality and that can be rapidly reorganized in response to signals such as auxin. Actin microfilaments as dynamic, axial, and even polar structures are therefore prime candidates for such a directional mechanism. In most elongating plant cells, actin is organized into longitudinal strands that reflect the cell axis (Parthasarathy et al. 1985), suggesting a role of actin for axial growth. In fact, disruption of the actomyosin system was shown to interfere with the maintenance of a growth axis in roots of thale cress (Baskin and Bivens 1995), and auxin was observed to reduce the rigor of the actin lattice in soybean root cells (Grabski and Schindler 1996). In

* Correspondence and reprints: Institut für Biologie II, Albert-Ludwigs-Universität Freiburg, Schänzlestrasse 1, 79104 Freiburg, Federal Republic of Germany.

coleoptiles, it has been known since long that auxin stimulates cytoplasmic streaming (Sweeney and Thimann 1937), motivating investigations where the inhibitory effect of certain divalent cations could be correlated to a disturbed assembly of actin microfilaments (Thimann and Biradivolu 1994).

In maize coleoptiles, cell elongation can be manipulated by activation of the plant photoreceptor phytochrome (Waller and Nick 1997) accompanied by a transition between two different arrays of actin: Microfilaments are organized in dense bundles in cells that elongate slowly. These bundles are split into fine strands when the cells enter accelerated elongation. Activation of the phytochrome system accelerates coleoptile expansion and the transformation of the dense microfilament bundles into fine strands. This response of actin was confined to the epidermis, i.e., to the tissue where growth control is located. Time course studies revealed that the response of microfilaments to light is fast and linked to corresponding changes of the growth rate (Waller and Nick 1997).

A similar actin response can be induced by auxin: Bundled microfilaments are characteristic for auxin-depleted cells, whereas the fine actin strands are formed upon addition of exogenous auxins (Wang and Nick 1998). In the rice mutant *Yin-Yang*, the fine strands persist during depletion from endogenous auxin. Upon addition of exogenous auxin, the actin cytoskeleton reorganizes into a perinuclear network in this mutant, and this becomes physiologically manifest as an auxin-inducible sensitivity of coleoptile growth to the actin-assembly blocker cytochalasin D (Wang and Nick 1998). Several aspects of the *Yin-Yang* phenotype such as precocious gravitropism or the formation of the perinuclear network of actin can be mimicked in the wild type by treatment with cytochalasin D. The analysis of this mutant led to a model, where auxin stimulates the dynamics of actin assembly and disassembly. The fine actin strands that are typical for auxin-rich cells and that are related to cell growth therefore represent a highly dynamic equilibrium between monomer addition and microfilament disassembly. In the mutant, this equilibrium collapses in response to auxin because monomer addition cannot keep pace with polymer disassembly.

These studies in coleoptiles suggest a role for actin in the control of cell growth. However, they raise two questions that stimulated the work presented here. (1) Actin filaments are organized in two distinct configurations. Is this mirrored in two pools of actin that are

biochemically distinguishable? (2) What is the functional link between the fine strands of actin and stimulated cell elongation on the one hand and bundled microfilaments and growth inhibition on the other?

Material and methods

Plant material

Seedlings of maize (*Zea mays* L. cv. Percival; Asgrow, Bruchsal, Federal Republic of Germany) were raised at 25 °C either in the dark or under continuous far-red light as described in detail in Waller and Nick (1997). The caryopses were soaked for 2 h in running tap water and sown equidistantly, embryo up, on moist cellulose (Pehazell; Hartmann, Heidenheim, Federal Republic of Germany). They were harvested at various time intervals after sowing for the experiments in Fig. 1. In the remaining experiments, the coleoptiles were used after four days of cultivation in far-red light.

Measurement of auxin-induced growth

Coleoptile segments (2 to 12 mm below the tip) were excised and the primary leaves carefully removed. To deplete the segments from endogenous auxin, they were incubated in water for 1 h in the dark at 25 ± 0.2 °C in a topover shaker at 20 rpm. Auxin (indolyl-3-acetic acid) was purchased from Fluka (Neu-Ulm, Federal Republic of Germany) and diluted freshly from an ethanolic stock solution (100 mM) that was stored in the dark at -20 °C. Following the depletion treatment, the segment tip was trimmed with a razor blade to adjust segment length to exactly 10 mm under dim green safelight (λ_{max} , 550 nm; 20 mW/m²), and the segments were then incubated in different concentrations of auxin for 3 h. In some experiments, brefeldin A (Sigma, Neu-Ulm, Federal Republic of Germany) at different concentrations diluted from a 5 mM stock solution in dimethyl sulfoxide (stored at -20 °C) was added together with the auxin. 0.1% (w/v) of ethanol and dimethyl sulfoxide were added into each assay to account for possible effects of the solvents and to equalize the samples for the highest solvent concentration used in the dose–response series. To minimize potential contamination by endogenous auxins or other endogenous factors originating from the coleoptiles themselves, both the depletion and the auxin incubation were performed at an excess volume of incubation medium (5 ml of medium for each segment). The length increment was measured at the end of the experiment and the segments were immediately frozen in liquid nitrogen for the assay of actin sedimentability. The length increment was calculated as percentage of the original segment length (10 mm). A value of 20% thus means that the segment has increased in length from 10 to 12 mm. Mean values and standard errors were plotted against the concentration of auxin or brefeldin A with typically 20–40 segments for each data point. The dose–response curves represent pooled data from two or three independent concentration series run at different days.

Assay for actin sedimentability

Following the measurement of growth, the segments were shock frozen and ground in a mortar in liquid nitrogen until a fine powder was obtained. The powder was thawed in ice-cold extraction buffer (25 mM morpholineethanesulfonic acid, 5 mM EGTA, 5 mM MgCl₂, 1 M glycerol, 1 mM GTP, 1 mM dithiothreitol, 0.25% [v/v] Triton X-100, 1 mM phenylmethylsulfonyl fluoride, 100 μM aprotinin, 10 μg of leupeptin and 10 μg of pepstatin per ml, pH 6.9) with 1 ml of buffer per g of fresh weight. The resulting suspension (defined as

total extract) was spun down at low speed (3000 g, 15 min, 4 °C), the supernatant transferred to fresh centrifuge tubes and centrifuged at high speed (20,000 g, 45 min, 4 °C) yielding a supernatant defined as soluble fraction and a sediment containing plasma membrane, endoplasmic reticulum, tonoplast, and Golgi membranes (Lützelshwab et al. 1988) defined as total-membrane fraction. In the resolubilization experiments, the total-membrane fraction was reconstituted with extraction buffer (using the same buffer volume as the supernatant that had been removed in the preceding step) supplemented either with potassium iodide (0.5 M) or with cytochalasin D (10 µM) or with Nonidet P-40 (1%, v/v) or with increasing concentrations of Triton X-100 (from 0.5%, v/v, in the control up to 1%, v/v). The sediment was carefully resuspended with a glass rod. After incubation on ice for 15 min, the residual-membrane fraction was collected by centrifugation at high speed (100,000 g, 10 min, 4 °C). Aliquots of total extract, soluble extract, total-membrane fractions, and residual-membrane fractions were mixed with two volumes of fresh, hot sample buffer (130 mM Tris-HCl, pH 6.5, 4% [w/v] sodium dodecyl sulfate, 10% [w/v] glycerol, 10% [v/v] 2-mercaptoethanol, 8 M urea) and incubated at 95 °C for 10 min. The samples were then ultrasonicated on ice for 30 s and spun down for 10 min at 15,300 g at 4 °C. The supernatant was transferred into a fresh reaction tube, frozen in liquid nitrogen, and stored until analysis at -20 °C. Protein concentrations were determined directly in the processed samples by the amido black method (Popov et al. 1975), and the proteins were analyzed by conventional sodium dodecyl sulfate-polyacrylamide gel electrophoresis and Western blotting as described in Nick et al. (1995), loading 5 µg of total protein per lane. Actin was visualized on the blots with a bioluminescence system (ECL; Amersham-Pharmacia, Freiburg, Federal Republic of Germany) by a mouse monoclonal antibody directed against chicken muscle actin (Amersham-Pharmacia) and a secondary antibody that was conjugated to horseradish peroxidase (Sigma). After development, the X-ray films were subjected to densitometry using an integrated density macro of an image-processing software (Image J). For the time-course studies (Fig. 1), each experimental series was repeated independently at least six times, for the brefeldin-auxin dose-response curves, each series was repeated independently at least two to three times. To quantify actin sedimentability, the densitometric data were calibrated with a total extract of etiolated coleoptiles (cultivated for 4 days) as an internal standard. From these calibrated data, the ratio between sedimentable and soluble actin could be calculated.

Visualization of actin and the endomembrane system

Actin microfilaments were visualized after mild fixation (1.8%, w/v, paraformaldehyde for 15 min) by phalloidin conjugated with fluorescein isothiocyanate (Sigma) as described in detail in Waller and Nick (1997). To assess whether brefeldin A had penetrated into the cells, the endomembrane system was visualized after mild fixation (Waller and Nick 1997) using either rhodamine-6G-chloride (Molecular Probes, Leiden, Netherlands) at 10 µg/ml, a dye that in animal cells stains mitochondria but also the nuclear envelope and an extensive reticulate network (Terasaki et al. 1984) that was later shown to represent the endoplasmic reticulum (Terasaki and Reese 1992), or FM4-64 (Molecular Probes, Eugene, Oreg., U.S.A.), a dye that stains a Golgi-derived membrane fraction related to polar exocytosis (Belanger and Quatrano 2000), at a concentration of 1 µg/ml. For both dyes, the tissue was stained for 10 min at room temperature and then washed three times 5 min with water. Images were obtained by confocal laser scanning microscopy using an argon-krypton laser and a line-averaging algorithm based on 32 individual scans per image. To visualize fluorescein isothiocyanate-conjugated phalloidin an excitation wavelength of 488 nm, a beam splitter at 515 nm, and a barrier filter at 520 nm were used. To visualize

rhodamine-6G-chloride and FM4-64, an excitation at 568 nm, a beam splitter at 580 nm, and a barrier filter at 590 nm were selected.

Results

Sedimentability of actin changes with growth rate

The growth rate of maize coleoptiles can be manipulated by activating the photoreceptor phytochrome in the absence of photosynthesis by irradiation with continuous far-red light. In dark-grown seedlings, growth is accelerated until it reaches a constant rate that is more or less maintained for several days until the coleoptile is fully expanded (Fig. 1 A, left). Only from day 5.5 after sowing it slows down again. In contrast, upon activation of the phytochrome system, growth is elevated dramatically with a peak of 0.5 mm/h 3.5 days after sowing (Fig. 1 A, right). This rapid growth is not stable, however: From day 4 the coleoptiles virtually cease to elongate and the primary leaves pierce through the coleoptile tip soon afterwards. The subcellular partitioning of actin was followed through these growth responses (Fig. 1 E). Total extracts (Fig. 1 B) were compared to the respective high-speed soluble fractions (Fig. 1 C) and total-membrane fractions that had been obtained by differential centrifugation (Fig. 1 D). To decide whether the actin in the total-membrane fraction was sedimentable because it was associated with membranes or simply because it was assembled into persistent microfilaments, these fractions were subjected to resolubilization experiments (Fig. 1 E). The actin in the total-membrane fractions could be solubilized by addition of detergents such as Nonidet P-40 or Triton X-100, and by the chaotropic agent potassium iodide but not by cytochalasin D, a blocker of actin assembly. This suggests that the actin in the total-membrane fraction is sedimentable because it is bound to membranes. When actin was probed in total extracts obtained at different times of the growth response (Fig. 1 B), a gradual decrease is observed over time with a generally elevated amount of actin in etiolated over irradiated coleoptiles. However, a dramatically different pattern was observed in the soluble (Fig. 1 C) and the total-membrane (Fig. 1 D) fractions. In extracts from etiolated coleoptiles, the signal for soluble actin is rising dramatically between day 2 and 3 and remains at a high level up to day 5.5, when it decreases sharply (Fig. 1 C, left), whereas the actin in the total-membrane fraction is decreasing with time (Fig. 1 D, left). In extracts from irradiated coleoptiles, all actin is found in the soluble fraction (Fig. 1 C, right) up to day 3.5 but

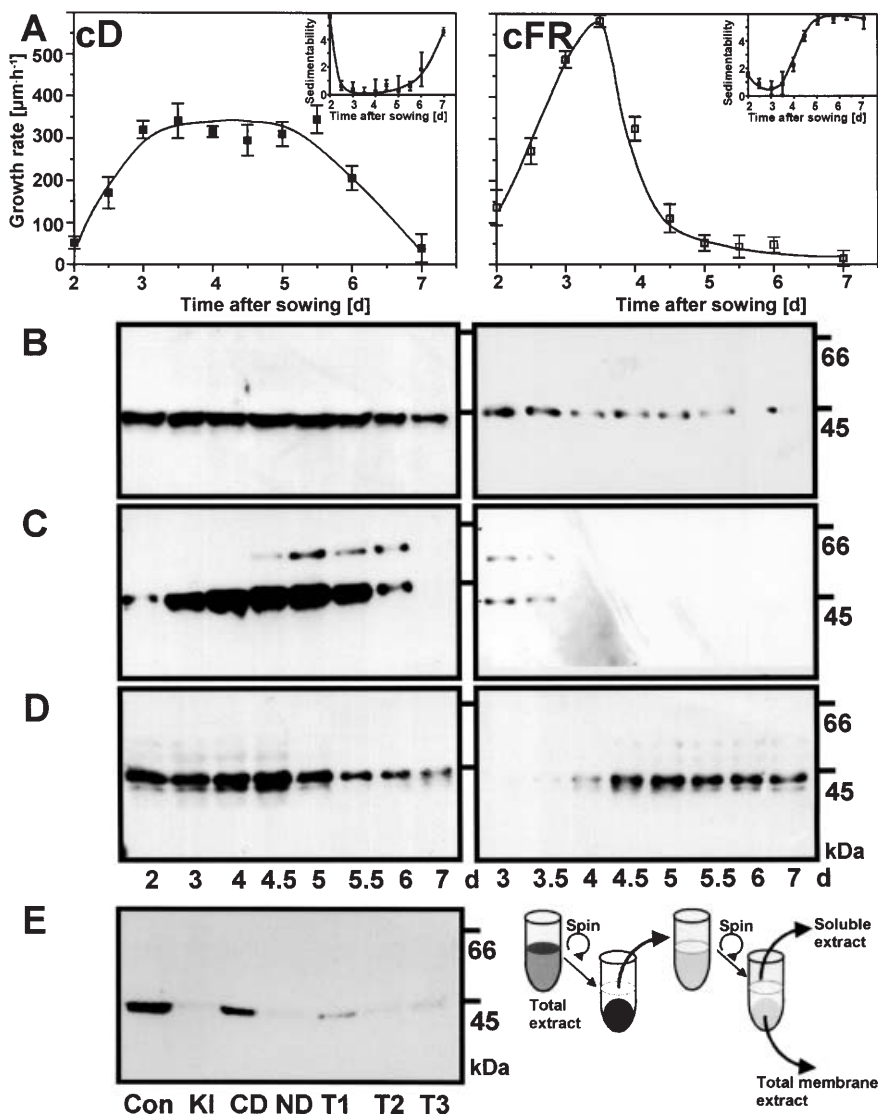


Fig. 1A–E. Changes of growth rate and the subcellular partitioning of actin in maize coleoptiles during cultivation in constant darkness (*cD*) or under constant far-red light (*cFR*). **A** Changes of growth rate over time. **Insets** Sedimentability of actin expressed as ratio between sedimentable versus soluble actin as quantified from densitometric data calibrated against an internal standard. **B–D** Changes of actin abundance in total extracts (**B**), in soluble fractions (**C**), and in total-membrane fractions (**D**). **E** Residual actin in the total-membrane fraction obtained from etiolated coleoptiles at day 4 after sowing after treatment with detergent or treatments that disassemble actin microfilaments with control (untreated total membrane fraction) (*Con*), 0.5 M potassium iodide (*KI*), 10 µM cytochalasin D (*CD*), 1% of Nonidet P-40 (*ND*), and 0.5%, 0.75% and 1% (v/v) of Triton X-100 (*T1*, *T2*, and *T3*, respectively). The fractionation protocol is schematically shown in the right-hand panel. 5 µg of total protein were loaded per lane in **B–E** and the fractions were challenged after electrotransfer with a monoclonal antibody against actin

completely shifted into the total-membrane fraction from day 4 (Fig. 1D, right).

When the sedimentability of actin is compared to growth rate (Fig. 1A, insets), a striking correlation emerges that holds for different light regimes and developmental stages: actin is more soluble in cells that elongate rapidly, it is found in the total-membrane fraction in cells that elongate slowly.

Sedimentability of actin and growth rate can be manipulated by brefeldin A

The stimulating effect of phytochrome on growth must be transmitted from the coleoptile tip (where phytochrome is located) to the elongating cells that are located several millimeters basal from the perceptive tissue. This stimulating signal can be mimicked by incu-

bation with the natural auxin indole-3-acetic acid (IAA) in coleoptile segments, where the perceptive tissue has been removed by decapitation (Fig. 2A). Growth is stimulated by IAA in concentrations up to 3 µM, whereas higher concentrations are less effective, leading to a typical, bell-shaped dose–response curve. When the dose–response curve of auxin-stimulated growth is measured in the presence of 0.3 µM of brefeldin A, a fungal drug that is widely used to block vesicle secretion, this bell-shaped dose–response curve is shifted by a factor of around 20–50 to higher concentrations (Fig. 2A). Growth is inhibited by brefeldin A for auxin concentrations that are below the optimum in the control (Fig. 2B, left and center), whereas it is stimulated for auxin concentrations that are supraoptimal in the control (Fig. 2B, right). The dose–response relation for these effects of brefeldin A

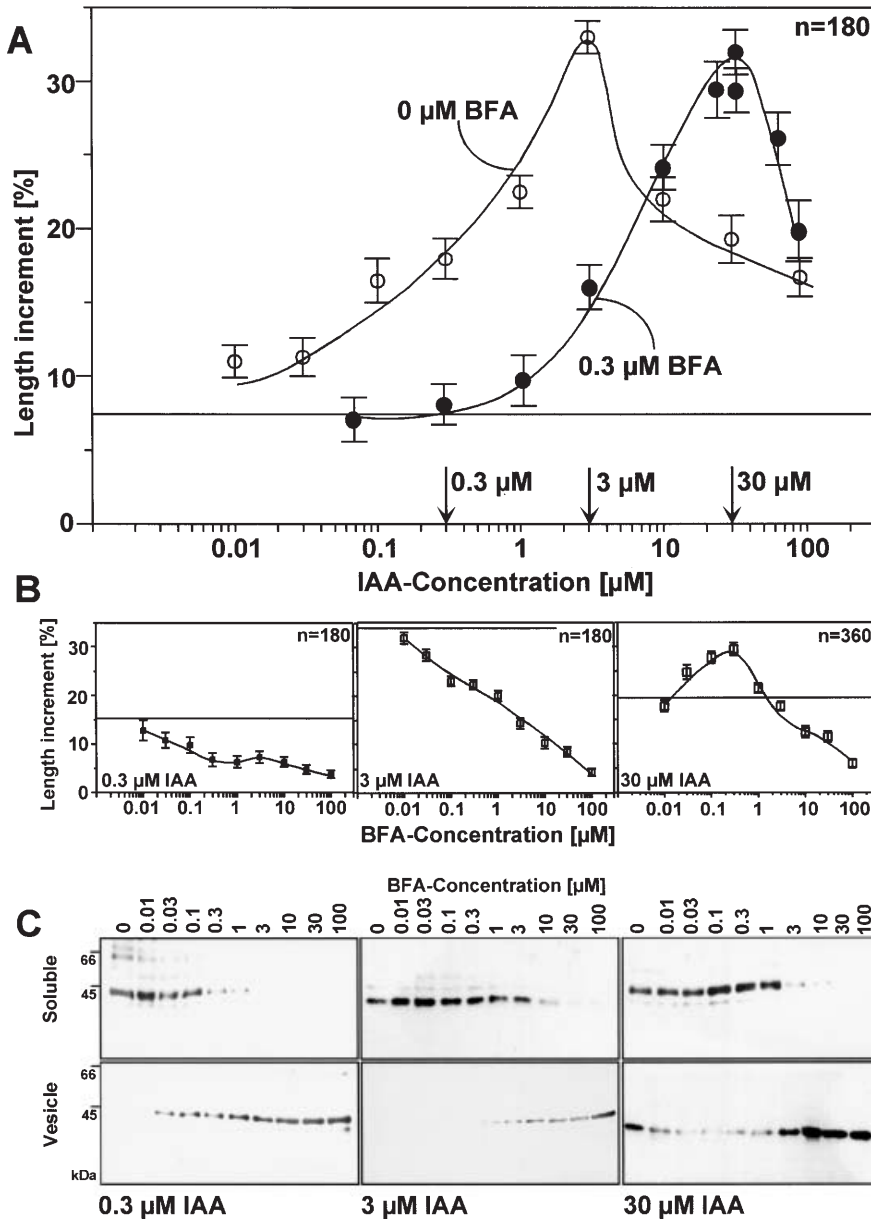


Fig. 2. Effect of brefeldin A on auxin-induced growth (**A** and **B**) of coleoptile segments and the subcellular partitioning of actin (**C**) in extracts obtained from the same segments. The length increment (in percent of the original length) was determined after 3 h at 25 °C. The segments were then shock frozen in liquid nitrogen and assayed for actin partitioning. **A** Dose–response curve of auxin-dependent growth in controls and in the presence of 0.3 μM brefeldin A. **B** Dose–response curve of the brefeldin A effect in the presence of a suboptimal (left), an optimal (center), and a supraoptimal (right) concentration of auxin. **C** Partitioning of actin between soluble and total-membrane fraction in relation to the concentration of brefeldin A in the presence of a sub-optimal (left), an optimal (center), and a supraoptimal (right) concentration of auxin. 5 μg of total protein loaded per lane

(Fig. 2B) showed that an extremely low concentration of 30 nM brefeldin A produced already a clear effect as compared to the controls. The membrane association of actin was assayed in the very segments that had been used for these dose–response curves and found to increase with increasing concentrations of brefeldin A for the low and for the optimal auxin concentration (Fig. 2C, left and center). Interestingly, for the supraoptimal auxin concentration (Fig. 2C, right), the membrane association of actin decreased for low concentrations of brefeldin A, whereas actin was repartitioned into the total-membrane fraction for concentrations exceeding 1 μM .

Summarizing these results, one can state that brefeldin A (1) shifts the dose–response curve of auxin-induced growth to higher concentrations, (2) alters the growth rate at very low concentrations, and (3) changes the sedimentability of actin in tight correlation with the observed changes of growth rate.

Actin is bundled in response to brefeldin A

To understand the increased sedimentability of actin in response to a treatment with brefeldin A, microfilaments were visualized after 15 min of incubation with brefeldin A in the presence of an auxin concentration

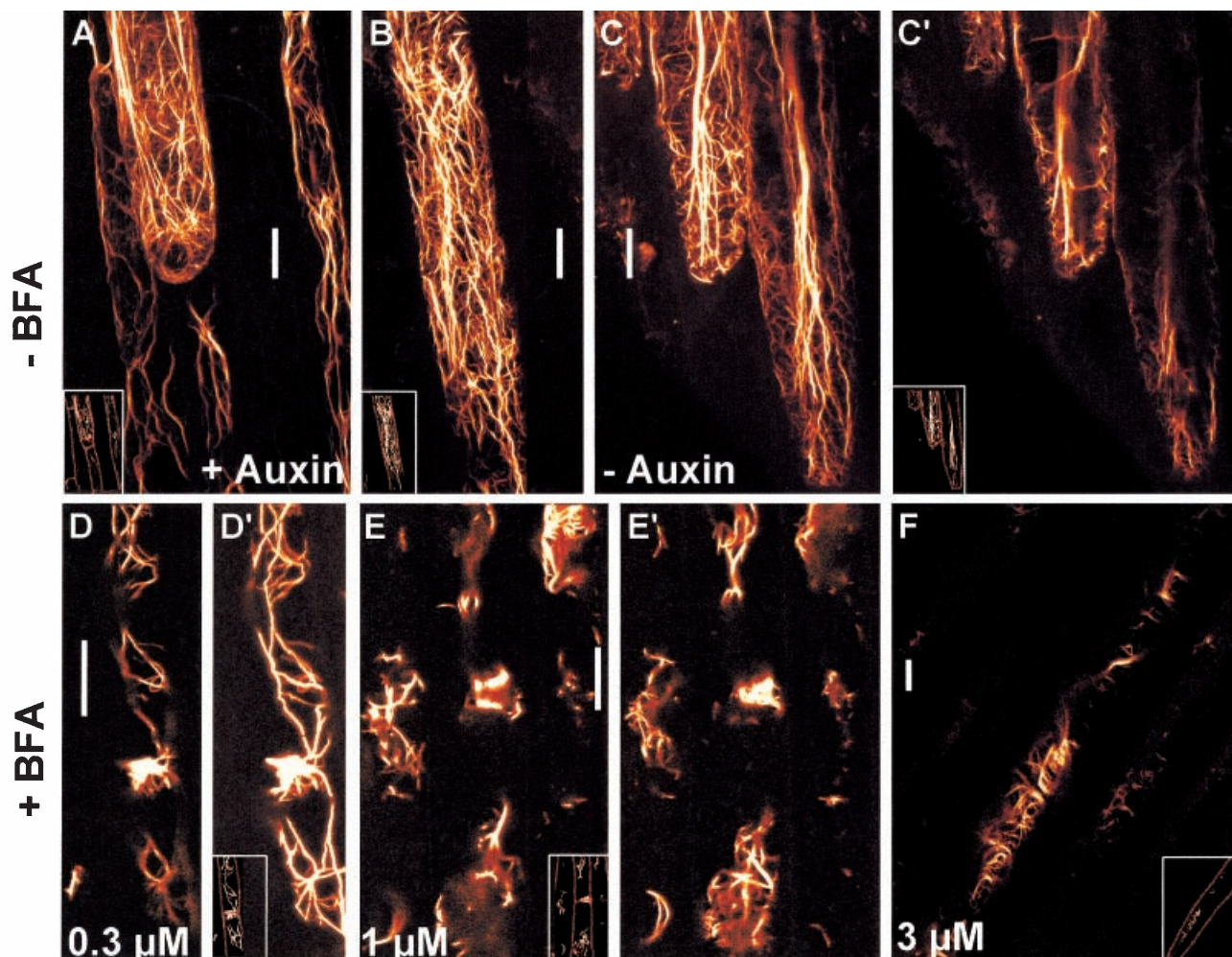


Fig. 3 A–F. Effect of auxin and brefeldin A on actin organization after incubation for 15 min at 25 °C. **A** and **B** Controls treated with 3 μM indole-acetic acid without brefeldin A showing the polar meshwork of actin (**A**) and the fine longitudinal actin strands (**B**). **C** and **C'** Two confocal sections of a cell that had been depleted from endogenous auxin by incubation in water. Note the bundling of longitudinal actin strands in the cell center. **D–F** Effect of brefeldin A on cells that were simultaneously treated with 3 μM indole-acetic acid. **D** and **D'** Two confocal sections showing agglomerations of actin in the cell pole after treatment with 300 nM brefeldin A. **E** and **E'** Two confocal sections showing the effect of a treatment with 1 μM brefeldin A. **F** Transverse actin bundles observed after treatment with 3 μM brefeldin A. Bar 10 μM. **Insets** Cell borders outlined

(3 μM) that was optimal for growth. In the absence of brefeldin A, microfilaments were observed to be organized in fine longitudinal strands (Fig. 3 A, B) that fanned out into a meshwork near the cell poles (Fig. 3 A). When auxin was washed out, these strands became bundled in the cell center (Fig. 3 C) and the polar meshwork emanating into the cell pole was found to weaken with only few filaments connecting the central bundles to the cell periphery (Fig. 3 C'). A similar response of actin could be induced in the presence of auxin when the cells were treated with very low (0.1 μM) concentrations of brefeldin A (data not shown). At slightly higher (0.3 and 1 μM brefeldin

A) concentrations, the polar meshwork of actin strands was replaced by dense agglomerations at the cell poles (Fig. 3 D, D', E, E'). In addition, numerous cortical actin microfilaments became trapped into meshlike arrays in the middle part of the cell (Fig. 3 E, E', F), especially at concentrations of 1 μM brefeldin A or higher, whereas the longitudinal actin bundles progressively disappeared.

Visualization of the endomembrane system with two fluorescent dyes under the same conditions to follow the effect of brefeldin A revealed that already low (0.1 μM) concentrations of brefeldin A caused significant changes in the structure of the endoplasmic

reticulum and the secretory apparatus (data not shown).

Discussion

Bundled microfilaments are correlated to vesicle-bound actin

In maize coleoptiles, cell elongation can be shifted over a wide range by activating the photoreceptor phytochrome (Fig. 1 A). These shifts of growth rate have been shown in a previous publication (Waller and Nick 1997) to be tightly correlated to changes in the organization of actin microfilaments in the coleoptile epidermis: Microfilaments were found to consist of fine parallel strands in rapidly elongating cells, whereas bundled microfilaments were typical for slowly elongating cells. Auxin, the central hormone in the control of coleoptile elongation, can control microfilament bundling in a similar way as light (Wang and Nick 1998). In the presence of auxin, microfilaments are organized in fine strands (Wang and Nick 1998) (Fig. 3 A, B) that are bundled in the cell center upon auxin depletion (Fig. 3 C, C'). The control of coleoptile elongation by phytochrome involves a control of auxin transport and auxin might thus be one of the transducers for light control (Furuya et al. 1969) along with auxin-independent pathways (Nick and Schäfer 1994). It is therefore possible that the actual signal for the light-induced bundling of actin microfilaments is a local depletion of auxin content.

Actin could be separated into a soluble fraction and into a subpopulation that cofractionated with the microsomal fraction (Fig. 1 E). This indicates that a part of actin is bound to membranes. Alternatively, the sedimentability of actin might be caused by bundles that persisted during the extraction procedure. To distinguish between these possibilities, the microsomal actin was subjected to a resolubilization assay using different compounds (Fig. 1 E). Actin could be resolubilized successfully by KI, a chaotropic agent that has been used to solubilize peripheral membrane proteins such as the naphthylphthalamic acid binding site (Cox and Muday 1994). However, a chaotropic agent is also expected to disassemble sedimentable protein polymers that are not bound to membranes. Cytochalasin D, a drug that eliminates actin strands (Cooper 1987), was not effective, suggesting that it is not bundling that is responsible for actin sedimentability. However, the effect of cytochalasin D depends on the dynamics of

actin assembly and disassembly. Microfilaments with a low dynamics might therefore resist a treatment of this drug even if they were not bound to membranes. The decisive experiment was therefore the successful resolubilization of sedimentable actin by detergents such as Nonidet P-40 and Triton X-100, demonstrating that the sedimentability of actin is caused by membrane association.

The relation between soluble and membrane-bound actin is regulated: In rapidly growing cells, where microfilaments are organized into fine strands, actin is preferentially found in the soluble fraction (Figs. 1 A, C and 2 C). In cells where elongation is impaired, actin is shifted into the total-membrane fraction (Figs. 1 A, D and 2 C).

Auxin sensitivity is maintained by active secretion

Brefeldin A shifts the dose–response curve for auxin-dependent cell elongation towards higher auxin concentrations (Fig. 2 A). This shift of sensitivity occurs in a dose-dependent manner with strong effects detectable already for a low (100 nM) concentration of brefeldin A (Fig. 2 B). When the effect of brefeldin A is assayed for a supraoptimal auxin concentration (30 μ M IAA), growth is stimulated for low concentrations of the drug (Fig. 2 B, right). This appears surprising at first sight but is consistent with a progressive shift of the optimum of the auxin dose–response curve towards higher auxin concentrations upon addition of brefeldin A.

When the subcellular fractionation of actin is investigated, actin is found to be partitioned from the soluble fraction into the total-membrane fraction with increasing concentrations of brefeldin A (Fig. 2 C). Again, for a supraoptimal auxin concentration (30 μ M IAA), this repartitioning is inverted, from the total-membrane fraction into the soluble fraction, for low concentrations of brefeldin A (Fig. 2 C, right). Thus, the membrane association of actin responds to brefeldin A in the same way as auxin sensitivity does.

With increasing concentration, brefeldin A produced the following effects in epidermal cells of coleoptiles that were supplied with an optimal (3 μ M) concentration of auxin (Fig. 3): a bundling of actin microfilaments (otherwise typical for auxin-depleted cells, Fig. 3 C, C'); the formation of actin aggregations at the poles of epidermal cells (Fig. 3 D, E); the formation of fused transverse filaments of cortical actin filaments in the middle portion of the cell (Fig. 3 F).

The treatment with the low concentrations of brefeldin A used in this study was sufficient to cause a swelling of the endoplasmic reticulum (data not shown). Brefeldin A is known to inhibit regulators of small G-proteins (ARF-GEF) that activate ADP-ribosylation factors (Arf) thus blocking secretion by interfering with the budding of Golgi vesicles (Orci et al. 1991). In consequence, the endomembrane system is expected to be blown up by the components that otherwise would be released into the periphery of the cell. This is accompanied by agglomerations of actin at the cell poles that are formed already at low concentrations of brefeldin A (Fig. 3 D, E). This is associated, on the physiological level, by a decrease of auxin sensitivity (Fig. 2 A), suggesting a relation between auxin sensitivity, the organization of actin microfilaments at the cell poles, and the endomembrane system.

This relation should be discussed in the context of recently published work on the role of ARF-GEFs, the molecular targets of brefeldin A, in auxin signaling. A treatment with brefeldin A caused a mislocalization of a cellular marker for polar auxin transport (Steinmann et al. 1999) mimicking the phenotype of a mutation in one of the ARF-GEFs. These findings suggest that a component essential for the function of the auxin system is not properly localized to the cell poles upon treatment with brefeldin A. Pilot experiments using radioactively labelled auxin (R. Godbolé et al., Universität Freiburg, Freiburg, Federal Republic of Germany, unpubl.) show an inhibition of polar auxin transport in coleoptiles by brefeldin A. This indicates that the drug interferes with the proper localization of auxin efflux carriers to the cell poles.

A role for actin in auxin signaling: ideas for a model

During the classical period of auxin research, Sweeney and Thimann (1937) proposed that auxin might induce coleoptile growth by stimulating cytoplasmic streaming that is indeed very prominent in the coleoptile epidermis. In a series of publications, Thimann returned to this idea and demonstrated a role of the actomyosin system, the molecular cause for cytoplasmic streaming, in coleoptile growth (Thimann et al. 1992, Thimann and Biradivolu 1994). Agents that interfere with actin polymerization block auxin-induced coleoptile growth at low concentrations, suggesting that the corresponding actin microfilaments are characterized by a highly dynamic equilibrium between assembly and disassembly (Thimann et al. 1992, Thimann and Biradivolu

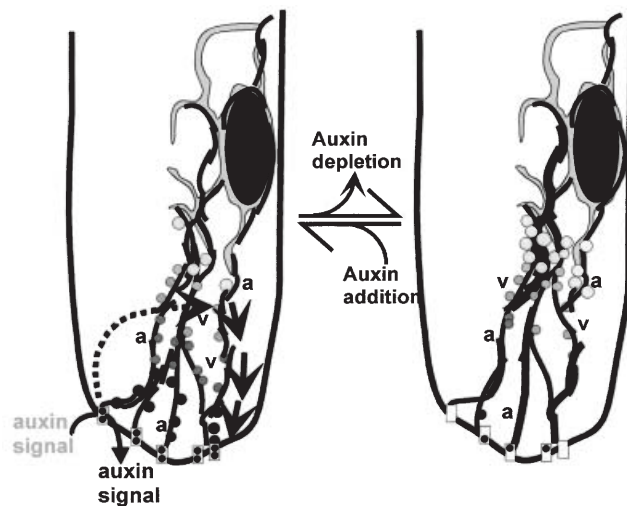


Fig. 4. Modell for the role of actin in auxin signaling. Actin microfilaments (*a*) move along the polar meshwork to the cell poles and carry as cargo vesicles (*v*) from the endoplasmic reticulum (gray) that contain elements necessary for the correct processing of the auxin signal. This transport is controlled by auxin. Upon auxin depletion, it is inhibited and the vesicles are trapped on the actin microfilaments

1994, Wang and Nick 1998). This conclusion was, at first sight, unexpected since actin was perceived as a lattice whose rigor confines cell growth with auxin stimulating growth by reducing this rigor (Grabski and Schindler 1996). In the framework of the actin-rigor model, the elimination of actin by actin polymerization blockers would be expected to stimulate rather than inhibit auxin-dependent growth.

The conclusions of the present study along with the findings of Thimann and coworkers suggest a different scenario for the function of actin (Fig. 4): microfilaments might transport vesicles towards the cell periphery, where they are released, especially near the polar region. This transport involves treadmilling in centrifugal direction (perhaps in combination with mutual sliding of actin microfilaments). This treadmilling and/or the release of the vesicles requires active auxin signaling. When the cells are depleted from auxin or when essential components of auxin signaling are mislocalized upon treatment with brefeldin A, the movement of actin is blocked, and the vesicles cannot be released in the cell periphery such that actin is trapped on the endomembrane system and partitioned into the total-membrane fraction (Figs. 1 and 2). The cellular manifestation of this trapping would be a bundling of actin strands into dense bundles. The cargo of these vesicles might be either components of auxin signaling

(such as auxin efflux carriers) or structural components of the cell wall. The observed association of actin with the cell poles (Fig. 3), i.e., with the slowly extending cross walls favors the scenario where the cargo consists in regulatory elements related to cell polarity such as the PIN1 protein that is discussed as the polar auxin efflux carrier (Gälweiler et al. 1998).

Outlook

The focus of future work will be on two questions.

How is the polarity of the vesicle transport maintained? If it is brought about by treadmilling of actin, there should be a gradient of actin-binding proteins that regulate the addition of actin monomers to the growing end of the filament and/or the disassembly at the shrinking end. If it is brought about by mutual sliding, there should be myosins that are influenced by auxin signalling.

What is the cargo of the vesicles? The cargo might be components necessary for signaling or components necessary for the growth response to this signaling. The plasma membrane of coleoptile cells has been estimated to be completely turned over within 3 h (Steer 1988), which means that it has to be replaced via guided vesicle traffic to the plasma membrane. The vesicles might also transport glycosyl residues for cell wall synthesis. Brefeldin A was shown to block, specifically and drastically, the incorporation of radioactively labeled glycosyl residues into the cell wall (Piro et al. 1999), suggesting that vesicle trafficking towards the cell periphery might be a very efficient target for growth control. Nevertheless, this general secretion is probably not a relevant target for the brefeldin A effects described in the present work since the cross walls, where the polar actin meshwork is directed to, grow only slowly. For this reason, the cargo of the vesicles transported to the cell poles probably contains components necessary for auxin signaling rather than components required for the growth response to auxin. Therefore, future work will involve a double visualization of actin and PIN1, the potential auxin efflux carrier (Gälweiler et al. 1998).

Acknowledgments

The present study was financed with funds from the Schwerpunktprogramm Molekulare Analyse der Phytohormonwirkung by the Deutsche Forschungsgemeinschaft (SPP Phytohormone) and by the Volkswagen-Stiftung (Nachwuchsgruppe Dynamik des pflanzlichen Zellskeletts).

References

- Baskin TI, Bivens NJ (1995) Stimulation of radial expansion in *Arabidopsis* roots by inhibitors of actomyosin and vesicle secretion but not by various inhibitors of metabolism. *Planta* 197: 514–521
- Belanger KD, Quatrano RS (2000) Membrane recycling occurs during asymmetric tip growth and cell plate formation in *Fucus distichus* zygotes. *Protoplasma* 212: 24–37
- Bergfeld R, Speth V, Schopfer P (1988) Reorientation of microfilaments and microtubules at the outer epidermal wall of maize coleoptiles during auxin-mediated growth. *Bot Acta* 101: 57–67
- Cooper JA (1987) Effects of cytochalasin and phalloidin on actin. *J Cell Biol* 105: 1473–1478
- Cosgrove DJ, Li Zh-Ch (1993) Role of expansin in cell enlargement of oat coleoptiles. *Plant Physiol* 103: 1321–1328
- Cox DN, Muday GK (1994) NPA binding activity is peripheral to the plasma membrane and is associated with the cytoskeleton. *Plant Cell* 6: 1941–1953
- Furuya M, Pjon Ch-J, Fujii T, Ito M (1969) Phytochrome action in *Oryza sativa* L. III: the separation of photoperceptive site and growing zone in coleoptiles, and auxin transport as effector system. *Dev Growth Differ* 11: 62–76
- Gälweiler L, Guan CH, Muller A, Wisman E, Mendgen K, Yephremov A, Palme K (1998) Regulation of polar auxin transport by AtPIN1 in *Arabidopsis* vascular tissue. *Science* 282: 2226–2230
- Giddings TH, Staehelin A (1991) Microtubule-mediated control of microfibril deposition: a re-examination of the hypothesis. In: Lloyd CW (ed) *The cytoskeletal basis of plant growth and form*. Academic Press, London, pp 85–99
- Grabski S, Schindler M (1996) Auxins and cytokinins as antipodal modulators of elasticity within the actin network of plant cells. *Plant Physiol* 110: 965–970
- Kutschera U, Bergfeld R, Schopfer P (1987) Cooperation of epidermal and inner tissues in auxin-mediated growth of maize coleoptiles. *Planta* 170: 168–180
- Lützelshwab M, Asard H, Ingold U, Hertel R (1988) Heterogeneity of auxin-accumulating membrane vesicles from *Cucurbita* and *Zea*: a possible reflection of cell polarity. *Planta* 177: 304–311
- McDougall GJ, Fry SC (1988) Inhibition of auxin-stimulated growth of pea stem segments by a specific nonasaccharide of xyloglucan. *Planta* 175: 412–416
- Nick P, Schäfer E (1994) Polarity induction versus phototropism in maize: auxin cannot replace blue light. *Planta* 195: 63–69
- Bergfeld R, Schäfer E, Schopfer P (1990) Unilateral reorientation of microtubules at the outer epidermal wall during photo- and gravitropic curvature of maize coleoptiles and sunflower hypocotyls. *Planta* 181: 162–168
- Schäfer E, Hertel R, Furuya M (1991) On the putative role of microtubules in gravitropism of maize coleoptiles. *Plant Cell Physiol* 32: 873–880
- Lambert AM, Vantard M (1995) A microtubule-associated protein in maize is induced during phytochrome-dependent cell elongation. *Plant J* 8: 835–844
- Orci L, Tagaya M, Amherdt M, Perrelet A, Donaldson JG, Lippincott-Schwartz J, Klausner RD, Rothman JE (1991) Brefeldin A, a drug that blocks secretion, prevents the assembly of non-clathrin-coated buds on Golgi cisternae. *Cell* 64: 1183–1195
- Parthasarathy MV, Perdue TD, Witztum A, Alvernaz J (1985) Actin network as a normal component of the cytoskeleton in many vascular plant cells. *Am J Bot* 72: 1318–1323
- Piro G, Montefusco A, Pacoda D, Dalessandro G (1999) Brefeldin A: a specific inhibitor of cell wall polysaccharide biosynthesis in oat coleoptile segments. *Plant Physiol Biochem* 37: 33–40

- Popov N, Schmitt S, Matthies H (1975) Eine störungsfreie Mikromethode zur Bestimmung des Proteingehaltes in Gewebematerialien. *Acta Biol Germ* 34: 1441–1446
- Rayle DL, Cleland RE (1992) The acid growth theory of auxin-induced cell elongation is alive and well. *Plant Physiol* 99: 1271–1274
- Steer MW (1988) Plasma membrane turnover in plant cells. *J Exp Bot* 39: 987–996
- Steinmann T, Geldner N, Grebe M, Mangold S, Jackson CL, Paris S, Gälweiler L, Palme K, Jürgens G (1999) Coordinated polar localization of auxin efflux carrier *PIN1* by *GNOM* ARF GEF. *Science* 286: 316–318
- Sweeney BM, Thimann KV (1937) The effect of auxin on cytoplasmic streaming. *J Gen Physiol* 21: 123–135
- Terasaki M, Reese TS (1992) Characterization of endoplasmic reticulum by co-localization of BiP and dicarbocyanine dyes. *J Cell Sci* 101: 315–322
- Song J, Wong JR, Weiss MJ, Chen LB (1984) Localization of endoplasmic reticulum in living and glutaraldehyde-fixed cells with fluorescent dyes. *Cell* 38: 101–108
- Thimann KV, Biradivolu R (1994) Actin and the elongation of plant cells II: the role of divalent ions. *Protoplasma* 183: 5–9
- Reese K, Nachmikas VT (1992) Actin and the elongation of plant cells. *Protoplasma* 171: 151–166
- Waller F, Nick P (1997) Response of actin microfilaments during phytochrome-controlled growth of maize seedlings. *Protoplasma* 200: 154–162
- Wang QY, Nick P (1998) The auxin response of actin is altered in the rice mutant *Yin-Yang*. *Protoplasma* 204: 22–33